bioRχiv

Neurodevelopmental clustering of gene expression identifies lipid metabolism genes associated with neuroprotection and neurodegeneration.

Akiva A. Kohane[a*] and Tim R. Wood[b]
[a]Gann Academy, Waltham, MA
[b]Broad Institute of Harvard and Massachusetts Institute of Technology, Cambridge, MA

*Correspondence should be addressed to A.A.K (akiva@kohane.org)

Abstract

APOE variants present the strongest association with sporadic Alzheimer's Disease. APOE is also highly expressed during neurodevelopment in the Central Nervous System (CNS) and has been shown to be neuroprotective in infancy and gestation. We explored other lipid metabolism genes to determine whether they show a similar neurodevelopmental expression trajectory and are associated with neurodegeneration. APOE was by far the most highly expressed of the lipid metabolism genes in the CNS. Two other genes, Apolipoprotein C1 (APOC1) Glutamate-Ammonia Ligase (GLUL—also known as glutamine synthetase), co-clustered with Apolipoprotein E (APOE) in its developmental trajectory in late gestation through early childhood. These three genes highlight brain structures and developmental time-windows distinct from other lipid metabolism genes. In the CNS they are primarily expressed in astrocytes and are implicated in neuroprotection and neurodegeneration.

Introduction

APOE is a lipoprotein involved in lipid metabolism with specific variants implicated through epidemiological and in vitro evidence with neurodegeneration [1]. The variant APOE4 has been repeatedly identified as the highest risk genetic factor for sporadic Alzheimer's disease as well as contributing to cardiovascular disease. Although primarily produced in the liver, APOE is also expressed in the CNS where it is mostly produced by astrocytes, much less by oligodendrocytres and microglia and even in neurons in specific pathological states[2]. In the CNS, APOE is the major apolipoprotein carrier of cholesterol and because of its role in generating HDL-like particles in the CNS it is also a major determinant of the distribution of phospholipids in the CNS. LDL Cholesterol itself is synthesized in the CNS from acetate and not imported from the periphery and the blood brain barrier prevents most lipids including cholesterol to enter the CNS. Lipids overall form 50% of the dry weight of the brain, second only to adipose tissue. Of that dry weight glycerophosphatides account for approximately 20% in gray matter and white matter and 78% in myelin. Cholesterol accounts for 8% in the gray matter, 15% in white matter and 20% in myelin. [3].

Given the centrality of lipids and cholesterol in the composition of the human brain, the abundance of APOE in the CNS, the growing evidence that cholesterol and lipid metabolism disorders have been implicated in several neurodevelopmental disorders some rare [4] and others more common (e.g. ADHD)[5,6], we sought to investigate which lipid metabolism genes had similar neurodevelopmental trajectories to APOE to determine which could be implicated in both neurodevelopmental processes and neurodegenerative diseases. This guilt-by-association strategy was enabled by the availability of transcriptome-wide data sets, specifically the Brainspan data set generated as part of the Allen Brain Atlas [7]. This data set provides transcriptomic measures at multiple developmental stages and in multiple defined structures of the CNS. We used an unsupervised learning/clustering approach across these tissues and developmental states to find the closest neighbors in tissue and developmental state trajectories.

Results

First subheading has no extra space before it

APOE is the most highly expressed gene of all the 103 gene lipid metabolism panel. As illustrated by the heatmap in Figure 1, it is expressed at one to two orders of magnitude higher levels than most of the other panel genes during embryogenesis to age 40 years. The higher levels of expression start at approximately 25 post-conceptual weeks (pcw) and continue to rise through age 2 years and then return to much lower expression levels before age 30 years as illustrated in Figure 2. Most of the neocortex follows this expression pattern but the highest APOE expression levels occur in the thalamus. The trajectory for hippocampus and striatum APOE expression follows a similar pattern but at lower levels.

The gene expression profiles of the lipid panel were analyzed by non-negative matrix factorization to generate two unsupervised clusters (see Methods, below). Each column in the W matrix corresponds to a cluster and each row the coefficient of a gene. APOE has the highest coefficient in Column 0 (see Supplementary Figure S1b)—cluster C0. The coefficient of APOE in C0 was two orders of magnitude higher than most of the lipid panel genes. The next most highly ranked genes in C0 are GLUL and APOC1. Like APOE their coefficients in column 0 of the W matrix

are

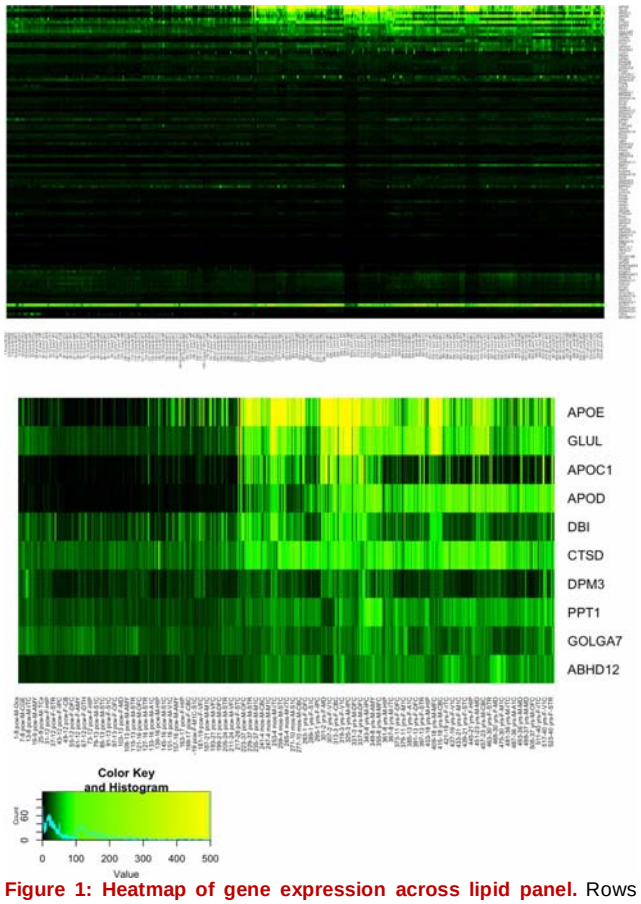

Figure 1: Heatmap of gene expression across lipid panel. Rows correspond to genes ordered by their coefficient in Column 0 of the NMF W matrix (descending from top to bottom) and the columns correspond to samples ordered by increasing age (left to right). The middle panel shows the top 10 genes in the topmost panel for clarity. The bottom panel is the color key and histogram of gene expression values.

Higher than in column 1. As shown in Supplementary Figure S3(a, b) they have similar trajectories to APOE. The C0 coefficient of the next highest ranked gene, APOD, is lower than that in C1 unlike the higher ranked genes (APOE, GLUL, APOC1). Therefore, it is not surprising that the APOD trajectory, across all samples, not just in C0, in Supplementary Figure S3© is markedly different from the first three trajectories described above. This is reflected in the correlation heatmap (Supplementary Figure S4) where the GLUL and APOC1 are the most tightly correlated with APOE (with $\boldsymbol{z}$ scores of 23.2 and 24.8 respectively) with APOD ($\boldsymbol{z}$ score 18.1) next most correlated.

The plots described above include all the samples in the data set. If instead we stratify the samples by their membership in C0 or C1, an obviously and consistently decreased APOE expression is seen (Supplementary Figure S2(a)) across C1 samples relative to C0 samples. This difference is also true for GLUL and APOC1 (not shown) and is associated with a highly overlapping set of samples as illustrated for APOE and GLUL in Supplementary Figure S2(b, c). A *t* test comparing the male to the female samples' expression levels was not significant with $p > 0.05$.

Querying the GWAS catalog[13] for the associations for Alzheimer's Disease/neurodegeneration (AD/ND) reveals the well-known association for APOE and the association for APOC1 which also has been previously reported and may also contributes to the APOE4 risk independent of its proximity to APOE [14]). There are no known significant GWAS associations between GLUL and AD/ND.

Discussion

Given the importance of lipids as constituents of brain structure and lipid metabolism in neurodevelopment and neurodegeneration, we undertook a unsupervised clustering study of lipid metabolism genes in the developing CNS. Within the two clusters obtained across developmental time and across tissues, three genes, APOE, APOC1 and GLUL were top ranked in one cluster and with the greatest difference with respect to the second cluster. Furthermore, APOE was most tightly correlated across the entire data set with the same two genes, all with p values $< 2.2 \times 10^{-16}$.

GLUL catalyzes the production of glutamine from glutamate and ammonia. Glutamine is a central metabolite in cellular energy balance including fatty acid synthesis particularly during hypoxia [15]. In the brain GLUL, mostly produced by astrocytes, eliminates neurotoxic glutamate and neurotoxic ammonia by synthesizing glutamine which is then taken up by glutamatergic neurons. Those neurons subsequently deamidate the glutamine to generate glutamate to serve energy metabolism or as neurotransmitter.

GLUL has been shown to be neuroprotective [16] during neurodevelopment in mopping up glutamate and ammonia both of which are neurotoxic. Independently, glutamine protects against cholesterol-dependent cytolysis [17]. Further glutamine blockade increases inflammatory signatures in microglia [18]. APOE is tightly regulated by processes of nerve degeneration and regeneration [19]. AD APOE risk alleles have been associated with differential pediatric gray matter maturation [20] as have responses to insults such as traumatic injury [21,22] and infections [23]. APOC1 suppresses glial inflammatory signaling and its expression is modulated downwards by the APOE ε4 AD risk allele [14].

Regarding neurodegeneration, APOE variants have been the most studied and demonstrated to contribute more to sporadic AD than any other variants. APOC1 has also been shown through eQTL analysis to have an independent contribution to AD risk, possibly through modulating APOE expression. GLUL variants have not been associated with AD. However, a recent mendelian randomization study supports the hypothesis of a neuroprotective effect of circulating glutamine regarding AD [24] . This suggests that prior findings of elevated expression of GLUL in brains of AD patients may be a compensatory rather than a pathogenetic mechanism [25].

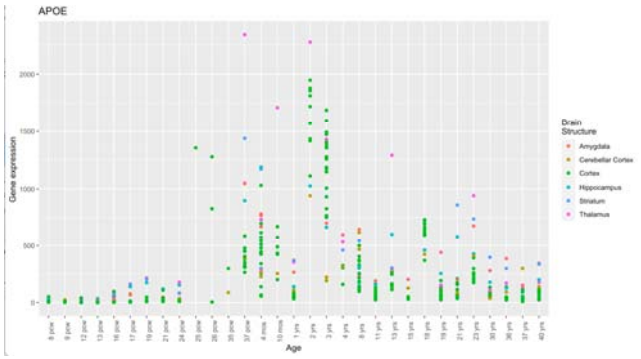

Figure 2: Structure- and Age-specific APOE expression.

In summary, three genes: —APOE APOC1 and GLUL—were highly expressed and highly correlated in a study of developmental gene expression in the brain. All three rise from 25 weeks pcw to age 3, most markedly in the neocortex and thalamus. Additionally, all three are known to be expressed preferentially in astrocytes compared to other CNS cells.

All three of these genes have been shown to have neuroprotective effects during neurodevelopment. Also, all three are also associated with neurodegeneration suggesting that the neuroprotective effects in gestation may be mechanistically related to neuroprotective effects during neurodegeneration. Although this study focused on lipid metabolism, it may be that other neurodevelopmental neuroprotective genes are also important in neurodegenerative processes.

Limitations

The heuristics developed to identify the relevant brain-expressed, developmental-disorder associated genes are described in Methods (below). Other genes might be identified by different heuristics and may also share the APOE, GLUL, APOC1 group trajectories. Further, there may be other characteristics of the patients that were not recorded in the metadata that might explain the observed clustering in the PCA and subsequently analyzed by NMD.

References

1. Puglielli L, Tanzi RE, Kovacs DM. Alzheimer's disease: the cholesterol connection. Nat Neurosci. 2003;6: 345–351. Doi:10.1038/nn0403-345
2. Mahley RW. Central Nervous System Lipoproteins: ApoE and Regulation of Cholesterol Metabolism. Arterioscler Thromb Vasc Biol. 2016;36: 1305–1315. Doi:10.1161/ATVBAHA.116.307023
3. O'Brien JS, Lois Sampson E. Lipid composition of the normal human brain: gray matter, white matter, and myelin *. J Lipid Res. 1965;6: 537–544. Doi:10.1016/S0022-2275(20)39619-X
4. Merkens LS, Wassif C, Healy K, Pappu AS, DeBarber AE, Penfield JA, et al. Smith-Lemli-Opitz syndrome and inborn errors of cholesterol synthesis: summary of the 2007 SLO/RSH Foundation scientific conference sponsored by the National Institutes of Health. Genet Med. 2009;11: 359–364. Doi:10.1097/GIM.0b013e31819b246e
5. Cartocci V, Servadio M, Trezza V, Pallottini V. Can Cholesterol Metabolism Modulation Affect Brain Function and Behavior? J Cell Physiol. 2017;232: 281–286. Doi:10.1002/jcp.25488
6. Chen T, Yuan H, Sun Y-B, Song Y-C, Lu M, Ni X, et al. Metabolomics study of the prefrontal cortex in a rat model of attention deficit hyperactivity disorder reveals the association between cholesterol metabolism disorder and hyperactive behavior. Biochem Biophys Res Commun. 2020;523: 315–321. Doi:10.1016/j.bbrc.2019.12.016
7. Miller JA, Ding S-L, Sunkin SM, Smith KA, Ng L, Szafer A, et al. Transcriptional landscape of the prenatal human brain. Nature. 2014;508: 199–206. Doi:10.1038/nature13185
8. Fagerberg L, Hallström BM, Oksvold P, Kampf C, Djureinovic D, Odeberg J, et al. Analysis of the human tissue-specific expression by genome-wide integration of transcriptomics and antibody-based proteomics. Mol Cell Proteomics. 2014;13: 397–406. Doi:10.1074/mcp.M113.035600
9. Chen H, Sharp BM. Content-rich biological network constructed by mining PubMed abstracts. BMC Bioinformatics. 2004;5: 147. Doi:10.1186/1471-2105-5-147
10. Wheeler DL, Chappey C, Lash AE, Leipe DD, Madden TL, Schuler GD, et al. Database resources of the National Center for Biotechnology Information. Nucleic Acids Res. 2000;28: 10–14. Available: https://www.ncbi.nlm.nih.gov/pubmed/10592169
11. Lee DD, Seung HS. Learning the parts of objects by non-negative matrix factorization. Nature. 1999;401: 788–791. Doi:10.1038/44565
12. sklearn.decomposition.NMF — scikit-learn 0.24.2 documentation. [cited 26 Aug 2021]. Available: https://scikit-learn.org/stable/modules/generated/sklearn.decomposition.NMF.html
13. MacArthur J, Bowler E, Cerezo M, Gil L, Hall P, Hastings E, et al. The new NHGRI-EBI Catalog of published genome-wide association studies (GWAS Catalog). Nucleic Acids Res. 2017;45: D896–D901. Doi:10.1093/nar/gkw1133
14. Cudaback E, Li X, Yang Y, Yoo T, Montine KS, Craft S, et al. Apolipoprotein C-I is an APOE genotype-dependent suppressor of glial activation. J Neuroinflammation. 2012;9: 192. Doi:10.1186/1742-2094-9-192
15. Brose SA, Marquardt AL, Golovko MY. Fatty acid biosynthesis from glutamate and glutamine is specifically induced in neuronal cells under hypoxia. J Neurochem. 2014;129: 400–412. Doi:10.1111/jnc.12617
16. Dossi E, Vasile F, Rouach N. Human astrocytes in the diseased brain. Brain Res Bull. 2018;136: 139–156. Doi:10.1016/j.brainresbull.2017.02.001
17. Turner ML, Owens SE, Sheldon IM. Glutamine supports the protection of tissue cells against the damage caused by cholesterol-dependent cytolysins from pathogenic bacteria. PloS One. 2020;15: e0219275. Doi:10.1371/journal.pone.0219275
18. Palmieri EM, Menga A, Lebrun A, Hooper DC, Butterfield DA, Mazzone M, et al. Blockade of Glutamine Synthetase Enhances Inflammatory Response in Microglial Cells. Antioxid Redox Signal. 2017;26: 351–363. Doi:10.1089/ars.2016.6715
19. Ignatius MJ, Gebicke-Härter PJ, Skene JH, Schilling JW, Weisgraber KH, Mahley RW, et al. Expression of apolipoprotein E during nerve degeneration and regeneration. Proc Natl Acad Sci U S A. 1986;83: 1125–1129. Doi:10.1073/pnas.83.4.1125
20. Chang L, Douet V, Bloss C, Lee K, Pritchett A, Jernigan TL, et al. Gray matter maturation and cognition in children with different APOE ε genotypes. Neurology. 2016;87: 585–594. Doi:10.1212/WNL.0000000000002939
21. Ariza M, Pueyo R, Matarín M del M, Junqué C, Mataró M, Clemente I, et al. Influence of APOE polymorphism on cognitive and behavioural outcome in moderate and severe traumatic brain injury. J Neurol Neurosurg Psychiatry. 2006;77: 1191–1193. Doi:10.1136/jnnp.2005.085167
22. Zhou W, Xu D, Peng X, Zhang Q, Jia J, Crutcher KA. Meta-analysis of APOE4 allele and outcome after traumatic brain injury. J Neurotrauma. 2008;25: 279–290. Doi:10.1089/neu.2007.0489
23. Urosevic N, Martins RN. Infection and Alzheimer's Disease: The APOE ε4 Connection and Lipid Metabolism. Journal of Alzheimer's Disease. 2008. Pp. 421–435. Doi:10.3233/jad-2008-13407
24. Adams CD. Circulating Glutamine and Alzheimer's Disease: A Mendelian Randomization Study. Clin Interv Aging. 2020;15: 185–193. Doi:10.2147/CIA.S239350
25. Robinson SR. Neuronal expression of glutamine synthetase in Alzheimer's disease indicates a profound impairment of metabolic interactions with astrocytes. Neurochem Int. 2000;36: 471–482. Doi:10.1016/s0197-0186(99)00150-3

Author contributions

A.A.K. conducted all the analyses and wrote the manuscript. T.R.W. suggested analytic techniques to cluster the expression data. He also provided insight regarding the connection between developmental signatures and neuroprotection vs neurodegeneration.

Competing interest statement

None of the authors report any competing interests.

Methods

Lipid Panel Selection

We curated a list of 103 genes—the "lipid panel"—(see Supplementary Table 1) involved in lipid metabolism which met the following criteria: 1) They were expressed in the brain as reported by a tissue-wide transcriptomic survey [8] with an expression level of at least 1 RPKM 2) They were associated in PubMed with lipid metabolism (using the Chilibot tool [9]) 3) They were associated with neurodevelopmental disorders as reported by the Online Mendelian Inheritance in Man database [10]

Gene Expression Data

Expression levels of each of those genes across multiple brain structures across development as measured in the Brainspan developmental transcriptome project (https://www.brainspan.org/) were downloaded. These gene-specific expression measures were previously described [7]. Some brain structures were sparsely represented across the Brainspan database and therefore therefore they were aggregated according to the mapping below.

BRAINSPAN STRUCTURE	AGGREGATED STRUCTURE
OCX	Cortex
M1C-S1C	Cortex
AMY	Amygdala
MGE	Cortex
STC	Cortex
URL	Cerebellar Cortex
CGE	Cortex
DTH	Thalamus
MFC	Cortex
DFC	Cortex
OFC	Cortex
LGE	Cortex
ITC	Cortex
HIP	Hippocampus
VFC	Cortex
PCX	Cortex
TCX	Cortex
A1C	Cortex
V1C	Cortex
STR	Striatum
M1C	Cortex
IPC	Cortex
S1C	Cortex
CB	Cerebellar Cortex
CBC	Cerebellar Cortex
MD	Thalamus

Table 1: Mapping Brainspan structures to a less sparse/more aggregated scheme.

Analysis

The gene expression measures were unit standard deviation normalized (see the Github repository at bit.ly/akivalipo for a Jupyter notebook with these analyses). Principal component analyses (PCA) revealed two clusters separated across PC1 (Supplementary Figure 1a). Non-Negative Matrix Factorization (NMF) [11] was used to determine the contributions of each gene to the clustering of the samples. Specifically, the original expression matrix $\boldsymbol{V}$ (with the columns representing samples and rows genes) is approximated with two smaller matrices $\mathbf{W}$ and $\mathbf{H}$ such that:

$$\mathbf{V} = \mathbf{WH}$$

The W matrix can be viewed as an archetype for each sample cluster with each column containing the coefficients for each gene for that cluster. NMF as implemented by the Python sci-kit library [12] was run with k=2 as informed by the two clusters seen in the PCA. Therefore, in this instance there are two columns in the W matrix. These are shown (Supplementary Figure 1b) for the top 10 genes ranked by their coefficients in column 0, along with the corresponding coefficients in column 1 and the absolute difference between the two columns shown in column 3.

(a)

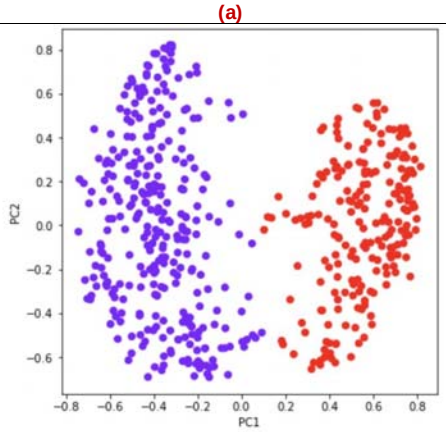

(b)

gene_symbol	0	1	absdiff
APOE	109.482649	0.000000	109.482649
GLUL	33.939569	14.955371	18.984197
APOC1	16.755972	0.269132	16.486840
APOD	7.059311	17.058865	9.999554
DBI	6.911500	7.026346	0.114846
CTSD	4.943901	20.599816	15.655915
DPM3	2.495586	4.806309	2.310723
PPT1	1.808399	11.648282	9.839884
GOLGA7	1.748346	8.808580	7.060233
ABHD12	1.422287	9.978674	8.556386

Supplementary Figure S1: Clustering of samples by expression values. (a) PCA of the unit normalized gene expression vectors for the samples results in two clusters divided across PC1. **(b)** Non-negative matrix factorization (NMF) sorted by the coefficients in column 0 with only the first 10 rows shown. Of those only the first three have coefficients larger in column 0 than in column 1.

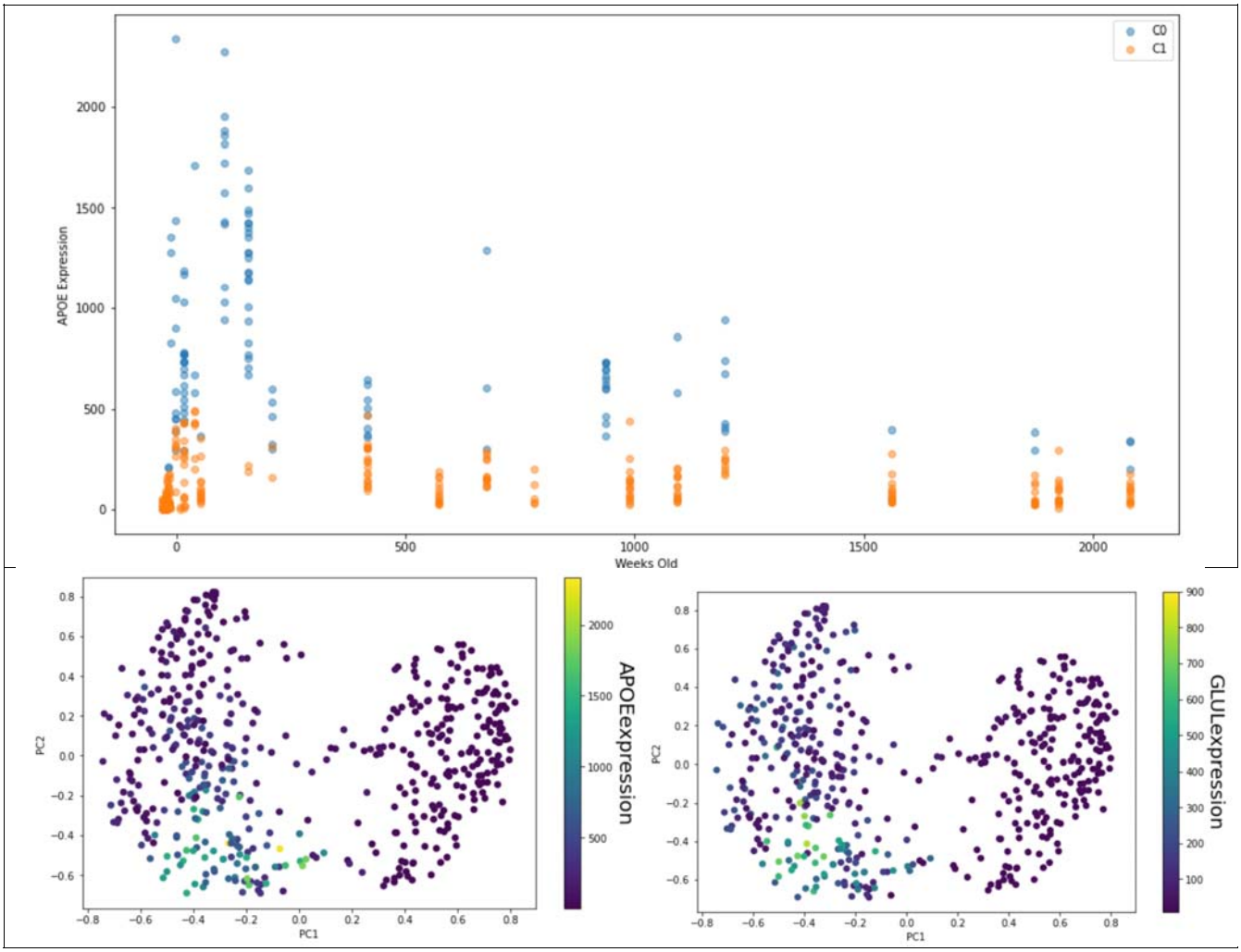

Supplementary Figure S2: Time series of the two clusters. (a) Time series of the two clusters showing the markedly higher expression of APOE in Cluster C0. **(b,c)** The strongest APOE and GLUL expression values overlap the same samples as shown by mapping the expression values onto the PCA of Figure S1(a).

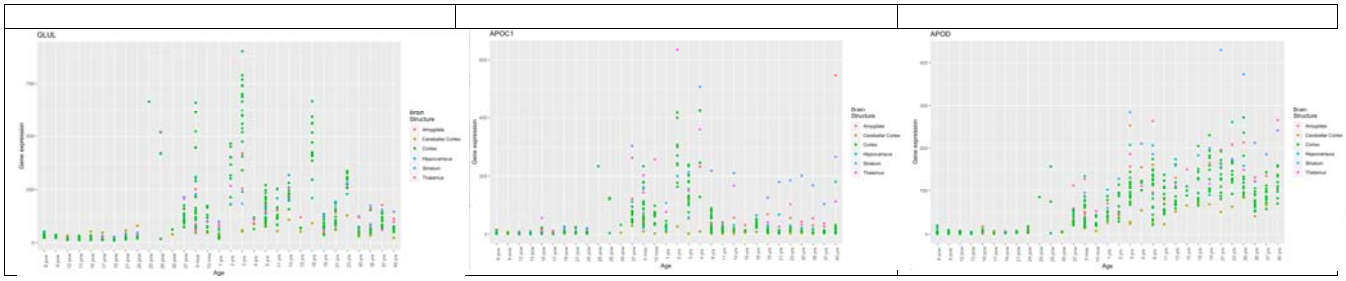

Supplementary Figure S3: Gene-specific expression pattern over age and brain structures. Note that these scatter plots include all the samples, not just those from one cluster. Each panel corresponds next hightest ranked genes in ***W*** matrix column 0 after APOE (which can be seen in Figure 1). **(a)** GLUL **(b)** APOC1 **(c)** APOD

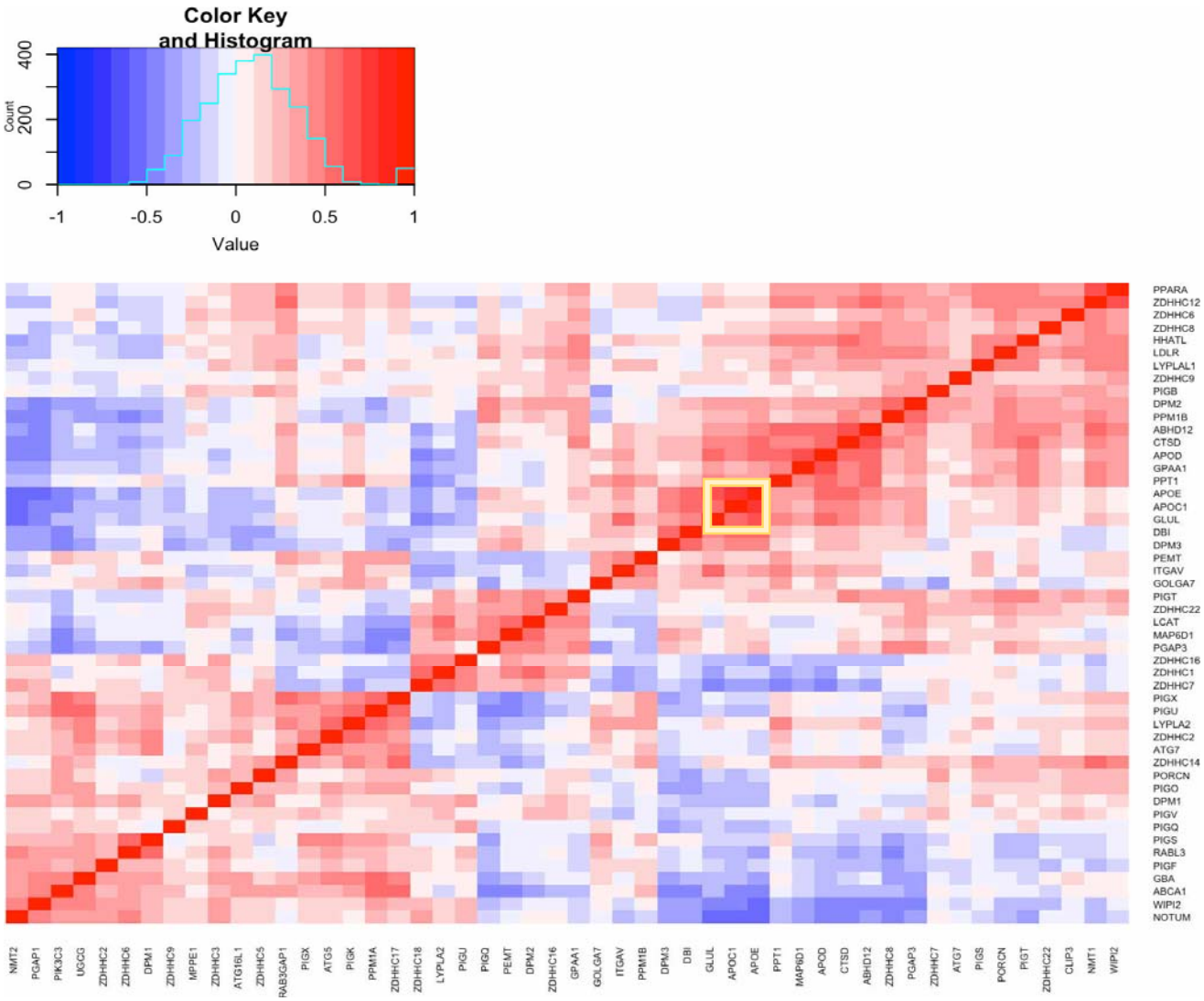

Supplementary Figure S4: Correlation matrix of lipid gene panel. All genes with median expression < 5 were eliminated to simplify the diagram and all samples were used to calculate the pairwise correlation matrix across genes using the Kendall rank correlation method for robustness. The complete linkage method was for hierarchical clustering and the dendrogram also omitted for simplicity of visualization. As quantified in the Results section, the genes with tightest correlation with APOE are GLUL and APOC1 (correlations outlined by yellow rectangle in the figure).

Supplementary Table 1

ensembl_gene_id	gene_symbol
ENSG00000165029	ABCA1
ENSG00000100997	ABHD12
ENSG00000139826	ABHD13
ENSG00000179477	ALOX12B
ENSG00000118137	APOA1
ENSG00000158874	APOA2
ENSG00000084674	APOB
ENSG00000111701	APOBEC1
ENSG00000130208	APOC1
ENSG00000110245	APOC3

ENSG00000189058	APOD
ENSG00000130203	APOE
ENSG00000204444	APOM
ENSG00000152348	ATG10
ENSG00000085978	ATG16L1
ENSG00000057663	ATG5
ENSG00000197548	ATG7
ENSG00000149311	ATM
ENSG00000105270	CLIP3
ENSG00000117984	CTSD
ENSG00000155368	DBI
ENSG00000062282	DGAT2
ENSG000000000419	DPM1
ENSG00000136908	DPM2
ENSG00000179085	DPM3
ENSG00000177628	GBA
ENSG00000135821	GLUL
ENSG00000147533	GOLGA7
ENSG00000197858	GPAA1
ENSG00000054392	HHAT
ENSG00000010282	HHATL
ENSG00000138448	ITGAV
ENSG00000259207	ITGB3
ENSG00000213398	LCAT
ENSG00000130164	LDLR
ENSG00000174697	LEP
ENSG00000101670	LIPG
ENSG00000120992	LYPLA1
ENSG00000011009	LYPLA2
ENSG00000143353	LYPLAL1
ENSG00000180834	MAP6D1
ENSG00000177669	MBOAT4
ENSG00000154889	MPPE1
ENSG00000138823	MTTP
ENSG00000136448	NMT1
ENSG00000152465	NMT2
ENSG00000185269	NOTUM
ENSG00000015520	NPC1L1
ENSG00000173391	OLR1
ENSG00000169174	PCSK9
ENSG00000133027	PEMT
ENSG00000197121	PGAP1
ENSG00000148985	PGAP2
ENSG00000161395	PGAP3
ENSG00000165195	PIGA

ENSG00000069943	PIGB
ENSG00000135845	PIGC
ENSG00000151665	PIGF
ENSG00000174227	PIGG
ENSG00000142892	PIGK
ENSG00000108474	PIGL
ENSG00000143315	PIGM
ENSG00000165282	PIGO
ENSG00000185808	PIGP
ENSG00000007541	PIGQ
ENSG00000087111	PIGS
ENSG00000124155	PIGT
ENSG00000101464	PIGU
ENSG00000060642	PIGV
ENSG00000163964	PIGX
ENSG00000119227	PIGZ
ENSG00000078142	PIK3C3
ENSG00000102312	PORCN
ENSG00000186951	PPARA
ENSG00000100614	PPM1A
ENSG00000138032	PPM1B
ENSG00000131238	PPT1
ENSG00000115839	RAB3GAP1
ENSG00000118873	RAB3GAP2
ENSG00000144840	RABL3
ENSG00000198168	SVIP
ENSG00000148154	UGCG
ENSG00000157954	WIPI2
ENSG00000159714	ZDHHC1
ENSG00000188818	ZDHHC11
ENSG00000160446	ZDHHC12
ENSG00000175048	ZDHHC14
ENSG00000102383	ZDHHC15
ENSG00000171307	ZDHHC16
ENSG00000186908	ZDHHC17
ENSG00000204160	ZDHHC18
ENSG00000163958	ZDHHC19
ENSG00000104219	ZDHHC2
ENSG00000180776	ZDHHC20
ENSG00000175893	ZDHHC21
ENSG00000177108	ZDHHC22
ENSG00000184307	ZDHHC23
ENSG00000163812	ZDHHC3
ENSG00000156599	ZDHHC5
ENSG00000023041	ZDHHC6

ENSG00000153786	**ZDHHC7**
ENSG00000099904	**ZDHHC8**
ENSG00000188706	**ZDHHC9**
ensembl_gene_id	**gene_symbol**
ENSG00000165029	ABCA1
ENSG00000100997	ABHD12
ENSG00000139826	ABHD13
ENSG00000179477	ALOX12B
ENSG00000118137	APOA1
ENSG00000158874	APOA2
ENSG00000084674	APOB
ENSG00000111701	APOBEC1
ENSG00000130208	APOC1
ENSG00000110245	APOC3
ENSG00000189058	APOD
ENSG00000130203	APOE
ENSG00000204444	APOM
ENSG00000152348	ATG10
ENSG00000085978	ATG16L1
ENSG00000057663	ATG5
ENSG00000197548	ATG7
ENSG00000149311	ATM
ENSG00000105270	CLIP3
ENSG00000117984	CTSD
ENSG00000155368	DBI
ENSG00000062282	DGAT2
ENSG00000000419	DPM1
ENSG00000136908	DPM2
ENSG00000179085	DPM3
ENSG00000177628	GBA
ENSG00000135821	GLUL
ENSG00000147533	GOLGA7
ENSG00000197858	GPAA1
ENSG00000054392	HHAT
ENSG00000010282	HHATL
ENSG00000138448	ITGAV
ENSG00000259207	ITGB3
ENSG00000213398	LCAT
ENSG00000130164	LDLR
ENSG00000174697	LEP
ENSG00000101670	LIPG
ENSG00000120992	LYPLA1
ENSG00000011009	LYPLA2
ENSG00000143353	LYPLAL1
ENSG00000180834	MAP6D1

ENSG00000177669	MBOAT4
ENSG00000154889	MPPE1
ENSG00000138823	MTTP
ENSG00000136448	NMT1
ENSG00000152465	NMT2
ENSG00000185269	NOTUM
ENSG00000015520	NPC1L1
ENSG00000173391	OLR1
ENSG00000169174	PCSK9
ENSG00000133027	PEMT
ENSG00000197121	PGAP1
ENSG00000148985	PGAP2
ENSG00000161395	PGAP3
ENSG00000165195	PIGA
ENSG00000069943	PIGB
ENSG00000135845	PIGC
ENSG00000151665	PIGF
ENSG00000174227	PIGG
ENSG00000142892	PIGK
ENSG00000108474	PIGL
ENSG00000143315	PIGM
ENSG00000165282	PIGO
ENSG00000185808	PIGP
ENSG00000007541	PIGQ
ENSG00000087111	PIGS
ENSG00000124155	PIGT
ENSG00000101464	PIGU
ENSG00000060642	PIGV
ENSG00000163964	PIGX
ENSG00000119227	PIGZ
ENSG00000078142	PIK3C3
ENSG00000102312	PORCN
ENSG00000186951	PPARA
ENSG00000100614	PPM1A
ENSG00000138032	PPM1B
ENSG00000131238	PPT1
ENSG00000115839	RAB3GAP1
ENSG00000118873	RAB3GAP2
ENSG00000144840	RABL3
ENSG00000198168	SVIP
ENSG00000148154	UGCG
ENSG00000157954	WIPI2
ENSG00000159714	ZDHHC1
ENSG00000188818	ZDHHC11
ENSG00000160446	ZDHHC12

ENSG00000175048	ZDHHC14
ENSG00000102383	ZDHHC15
ENSG00000171307	ZDHHC16
ENSG00000186908	ZDHHC17
ENSG00000204160	ZDHHC18
ENSG00000163958	ZDHHC19
ENSG00000104219	ZDHHC2
ENSG00000180776	ZDHHC20
ENSG00000175893	ZDHHC21
ENSG00000177108	ZDHHC22
ENSG00000184307	ZDHHC23
ENSG00000163812	ZDHHC3
ENSG00000156599	ZDHHC5
ENSG00000023041	ZDHHC6
ENSG00000153786	ZDHHC7
ENSG00000099904	ZDHHC8
ENSG00000188706	ZDHHC9